MITSUBISHI ELECTRIC RESEARCH LABORATORIES
http://www.merl.com

Spatial Scattering Modulation for Uplink Millimeter-Wave Systems

Ding, Y.; Kim, K.J.; Koike-Akino, T.; Pajovic, M.; Wang, P.; Orlik, P.V.

TR2017-071 June 2017

Abstract

In this letter, a new spatial scattering modulation (SSM) is proposed for uplink millimeter-wave (mmWave) systems that support a single user terminal (UT). By utilizing the analog and hybrid beamforming with a large antenna array and phase shifters for mmWave communications systems, an architecture where the UT has a single radio frequency (RF) chain, whereas the base station (BS) has more than one RF chains is adopted. In this architecture, the proposed SSM modulates some information bits on the spatial directions of scattering clusters in the angular domain, so that a higher spectral efficiency can be achieved with the use of a lower order modulation. For a particular number of scattering clusters and number of RF chains, a closed-form expression for the upper bound on the bit error rate (BER) is derived for the proposed SSM. Monte-Carlo simulations are also conducted to verify the achievable BER performance.

IEEE Communications Letters

Spatial Scattering Modulation for Uplink Millimeter-Wave Systems

Yacong Ding, Kyeong Jin Kim, Toshiaki Koike-Akino, Milutin Pajovic, Pu Wang, and Philip Orlik

Abstract—**In this letter, a new spatial scattering modulation (SSM) is proposed for uplink millimeter-wave (mmWave) systems that support a single user terminal (UT). By utilizing the analog and hybrid beamforming with a large antenna array and phase shifters for mmWave communications systems, an architecture where the UT has a single radio frequency (RF) chain, whereas the base station (BS) has more than one RF chains is adopted. In this architecture, the proposed SSM modulates some information bits on the spatial directions of scattering clusters in the angular domain, so that a higher spectral efficiency can be achieved with the use of a lower order modulation. For a particular number of scattering clusters and number of RF chains, a closed-form expression for the upper bound on the bit error rate (BER) is derived for the proposed SSM. Monte-Carlo simulations are also conducted to verify the achievable BER performance.**

Index Terms—**Spatial scattering modulation, millimeter-wave communication, analog beamforming, antenna array.**

I. Introduction

DUE to a high data rate demand in wireless communications, millimeter-wave (mmWave) band has received increased attention in recent years because of its large available bandwidth. Signals in the mmWave band experience more severe path loss than microwave signals. Thanks to a smaller wavelength, it is possible to pack more antenna elements in a given area, so that a beamforming technique can be leveraged to achieve a higher beamforming gain in combating the severe path loss. Due to high hardware cost and power consumption of radio frequency (RF) chains, it is impractical to equip every antenna element in a large array with a separate RF chain. Various architectures have been proposed for both analog beamforming and hybrid analog-digital precoding in mmWave systems [1].

In this paper, we employ a large antenna array at both the user terminal (UT) and base station (BS), so that a very narrow and directional beam can be formed to transmit signals in the uplink direction [2]. Motivated by the spatial modulation (SM) [3], we propose the spatial scattering modulation (SSM) that utilizes the spatial dimension of the antenna array in modulating a part of information on directions of scattering clusters in the angular domain. That is, the information is not only transmitted by modulated symbols, but also by the indices of the corresponding scattering clusters. The mmWave system based on SM concept has been proposed in [4] and [5], where a line-of-sight (LoS) scenario is considered in [4] and a generalized SM scheme is proposed in [5] with analog beamforming. In contrast to preexisting work, our main contributions are summarized as follows:

- We consider a non-line-of-sight (nLoS) scenario and propose a new modulation scheme (SSM) for the uplink mmWave system, where additional information bits are modulated on the indices of the scattering clusters. The proposed scheme is able to achieve a higher spectral efficiency with a limited number of RF chains at the UT.
- Using a simplified narrowband clustered channel model [6], [7], we verify the performance of the proposed uplink mmWave system using the bit error rate (BER) as a metric. To justify our BER performance, we compare it with that obtained by the theoretical upper bound on the BER. We also compare the BER performance with non-SSM-based maximum beamforming and random beamforming.

II. Spatial Scattering Modulation

A. Transmitter and Receiver Architecture

To combat severe path loss in mmWave band, it is required that the numbers of antenna elements N_r at the BS and N_t at the UT are large to achieve a high beamforming gain. Since it is impractical to apply an RF chain to each antenna element due to hardware cost and power consumption, we assume that only a single RF chain is employed at the UT in the uplink transmission. In this architecture, the RF chain is connected to all antenna elements in the array through a set of phase shifters. The BS, which acts as the receiver, has more sophisticated hardware and can afford more power consumption. Thus, we assume that the BS has multiple RF chains, and each of them is also connected to all antenna elements through its own set of phase shifters. These two architectures shown in Fig. 1 correspond to the analog and hybrid architectures in [8]. Since only one RF chain is available at the UT, only a single stream can be transmitted and the beamforming strategy is to steer in the dominant path direction to achieve the highest signal-to-noise ratio (SNR) at the end of the link [8]. In contrast, when the BS has $R \geq 2$ RF chains, a variety of analog-digital combining strategies can be employed as shown in [9]. Without any interference among scattering clusters and only a single stream transmission, the maximum ratio combining at the receiver will form its beam towards the scattering cluster which corresponds to the transmit beamforming direction.

Manuscript received February 17, 2017; accepted March 13, 2017. The associate editor coordinating the review of this paper and approving it for publication was G. Alexandropoulos.

Y. Ding is with Department of Electrical and Computer Engineering, University of California, San Diego, La Jolla, CA 92093.

K. J. Kim, T. Koike-Akino, M. Pajovic, P. Wang, and P. Orlik are with Mitsubishi Electric Research Labs (MERL), Cambridge, MA 02139, USA.

The work of Y. Ding was done while he was working at MERL.

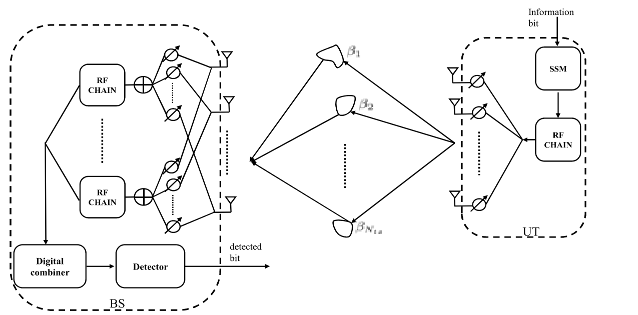

Fig. 1. Block diagram of the UT and BS in uplink communications, where β_l denotes the gain of the lth scattering cluster.

B. Channel Model

We adopt a narrowband discrete physical channel model [6], [7]. The channel matrix $\boldsymbol{H} \in \mathbb{C}^{N_r \times N_t}$ is assumed to be a sum of N_{ts} paths as follows:

$$\boldsymbol{H} = \sum_{l=1}^{N_{ts}} \beta_l \boldsymbol{a}_r(\theta_l^r) \boldsymbol{a}_t^H(\theta_l^t) \tag{1}$$

where β_l is the complex gain of the lth path, and θ_l^r and θ_l^t are azimuth angles of arrival (AoA) and angles of departure (AoD), respectively. We assume that both the UT and BS utilize a uniform linear array (ULA), so that the array manifold vectors $\boldsymbol{a}_r(\theta_l^r)$ and $\boldsymbol{a}_t^H(\theta_l^t)$ can be written as [2]:

$$\boldsymbol{a}_r(\theta_l^r) = \frac{1}{\sqrt{N_r}}\big[1, e^{j2\pi\psi_l^r}, e^{j2\pi\psi_l^r \cdot 2}, \ldots, e^{j2\pi\psi_l^r \cdot (N_r-1)}\big]^T,$$
$$\boldsymbol{a}_t(\theta_l^t) = \frac{1}{\sqrt{N_t}}\big[1, e^{j2\pi\psi_l^t}, e^{j2\pi\psi_l^t \cdot 2}, \ldots, e^{j2\pi\psi_l^t \cdot (N_t-1)}\big]^T$$

where $\psi_l^r \stackrel{\triangle}{=} \frac{d_r}{\lambda}\sin(\theta_l^r)$ and $\psi_l^t \stackrel{\triangle}{=} \frac{d_t}{\lambda}\sin(\theta_l^t)$, d_r, d_t denote antenna spacing at the receiver and transmitter, respectively, λ is the wavelength of the propagation. The channel model in (1) is a simplified version of the clustered channel model in [7]. Namely, we use a representative path to denote the total effects of all paths in a cluster.

When N_r and N_t are large, the beams are narrow, which, in turn, implies an approximate orthogonality, so that we have $\boldsymbol{a}_r(\theta_l^r)^H \boldsymbol{a}_r(\theta_k^r) \approx 0, l \neq k$ and $\boldsymbol{a}_t(\theta_l^t)^H \boldsymbol{a}_t(\theta_k^t) \approx 0, l \neq k$ [2], [6], [7]. This also implies that interference among scattering clusters is limited. Thus, in this paper, we assume an exact orthogonality among all AoA's and AoD's, formally as:

$$\boldsymbol{a}_r(\theta_l^r)^H \boldsymbol{a}_r(\theta_k^r) = \delta(l-k), \quad \boldsymbol{a}_t(\theta_l^t)^H \boldsymbol{a}_t(\theta_k^t) = \delta(l-k) \tag{2}$$

where $\delta(\cdot)$ denotes the Dirac delta function. This assumption is utilized to simply the theoretical calculations in this paper.

C. SSM Transmission

In SSM, rather than choosing the dominant direction for beamforming, the UT will form a beam to the direction determined by information bits. Out of N_{ts} scattering clusters, the UT chooses $N_s \leq R$ scattering clusters which have the largest cluster gains $|\beta_l|$ for possible transmission directions. Without loss of generality, we assume β_l with decreasing order of magnitude such that $|\beta_1| > |\beta_2| > \cdots > |\beta_{N_{ts}}|$. In each transmission, the first $\log_2(N_s)$ bits will be used to determine which one of the N_s scattering clusters the transmitter steers to. Then, the next $\log_2(M)$ bits will be utilized to determine the transmitted modulation symbol, where M denotes the constellation size. Denoting with s the transmitted symbol with unit power and $\boldsymbol{p} \in \mathbb{C}^{N_t \times 1}$ ($\|\boldsymbol{p}\|_2 = 1$) the transmitting direction, which also represents the weights of phase shifters, the received signal in the SSM transmission can be written as:

$$\boldsymbol{y} = \sqrt{E}\boldsymbol{H}\boldsymbol{p}s + \boldsymbol{n} \tag{3}$$

where $\boldsymbol{y} \in \mathbb{C}^{N_r \times 1}$ is the signal received at the receiver antennas, E is the transmission power, and $\boldsymbol{n} \sim \mathcal{CN}(\boldsymbol{0}, \sigma^2 \boldsymbol{I}_{N_r})$ is noise at receiver antennas. Also, $\mathcal{CN}(0, \sigma^2)$ denotes the circularly symmetric Gaussian distribution with variance σ^2.

1) One example of SSM with four scattering clusters, $N_s = 4$, and QPSK, $M = 4$, for modulation: For the random sequence of information bits $\boldsymbol{b} = [b_1, b_2, \ldots]$, we take every four bits ($\log_2(N_s) + \log_2(M)$) as a group, $[b_1, b_2, b_3, b_4]$. The following table shows the transmission scheme:

$[b_1 b_2]$	00	01	10	11
$\boldsymbol{p}$	$\boldsymbol{a}_t(\theta_1^t)$	$\boldsymbol{a}_t(\theta_2^t)$	$\boldsymbol{a}_t(\theta_3^t)$	$\boldsymbol{a}_t(\theta_4^t)$
$[b_3 b_4]$	00	01	10	11
s	$\frac{(1+1j)}{\sqrt{2}}$	$\frac{(1-1j)}{\sqrt{2}}$	$\frac{(-1+1j)}{\sqrt{2}}$	$\frac{(-1-1j)}{\sqrt{2}}$

Thus, for $[b_1, b_2, b_3, b_4] = [0\,0\,0\,0]$, (3) becomes

$$\begin{aligned}\boldsymbol{y} &= \sqrt{E}\Big(\sum_{l=1}^{N_{ts}} \beta_l \boldsymbol{a}_r(\theta_l^r) \boldsymbol{a}_t^H(\theta_l^t)\Big)\boldsymbol{a}_t(\theta_1^t)s + \boldsymbol{n} \\ &= \sqrt{E}\boldsymbol{a}_r(\theta_1^r)\beta_1(1+1j)/\sqrt{2} + \boldsymbol{n}.\end{aligned} \tag{4}$$

D. SSM Detection

The receiver signal $\boldsymbol{y}$ at the antenna array goes through the phase shifters, is combined and down converted by each RF chain. From (4), it shows that when the weights of the receiver phase shifter are $\boldsymbol{a}_r(\theta_k^r)$, where k corresponds to the transmission direction, the largest SNR can be achieved. However, the BS does not know which direction was used by the UT since this was determined by the random information bits. Thus, R RF chains are used at the receiver side to form beams towards all possible scattering clusters being used in the SSM. Denoting $\boldsymbol{r}_l$ as the phase shifter weights steering to the lth scattering cluster, we have

$$\boldsymbol{r}_{1:N_s} \stackrel{\triangle}{=} [\boldsymbol{r}_1, \ldots, \boldsymbol{r}_{N_s}] = [\boldsymbol{a}_r(\theta_1^r), \ldots, \boldsymbol{a}_r(\theta_{N_s}^r)]$$

and the signal after RF chain as:

$$\boldsymbol{y}_c = (\boldsymbol{r}_{1:N_s})^H \boldsymbol{y} = [\boldsymbol{a}_r(\theta_1^r)^H \boldsymbol{y}, \ldots, \boldsymbol{a}_r(\theta_{N_s}^r)^H \boldsymbol{y}]^T. \tag{5}$$

Notice that we require $R \geq N_s$ such that each RF chain can form a beam towards at least one scattering cluster. When $N_{ts} \geq R$, i.e., when we have more scattering clusters than the number of RF chains, we can choose up to R scattering clusters with largest gain magnitude to implement the SSM scheme. To decide which direction was used for transmission and which symbol was transmitted, we apply maximum likelihood (ML) detection as follows:

$$\{\hat{k}, \hat{s}\} = \mathop{\arg\min}_{\substack{k \in \{1, \ldots, N_s\}, \\ s}} |\boldsymbol{y}_c(k) - \boldsymbol{a}_r(\theta_k^r)^H \boldsymbol{H} \boldsymbol{a}_t(\theta_k^t)\sqrt{E}s|^2 \tag{6}$$

where $\hat{k}$ is the detected transmission direction which reveals the first $\log_2(N_s)$ bits, and $\hat{s}$ is the detected transmitted symbol representing the next $\log_2(M)$ bits. In this paper, we assume that perfect channel state information such as path gains (β_ls) and AoA/AoD (θ_l^r, θ_l^t) are known at the receiver, and the transmitter has access to them.

III. BER Performance Analysis

In this section, we derive the BER performance of the proposed SSM scheme. When channel gains $\beta_l, l = 1, \ldots, N_s$, are given, assume that k^* and s^* are true transmission direction and transmitted symbol, whereas $\hat{k}$ and $\hat{s}$ are detected direction and symbol using criterion in (6). Then the conditional pairwise error probability (CPEP) is given by

$$\begin{aligned} &\mathbb{P}\big(\{k^*, s^*\} \to \{\hat{k}, \hat{s}\} \mid \beta_1, \ldots, \beta_{N_s}\big) = \\ &\mathbb{P}\big(|\boldsymbol{y}_c(k^*) - \boldsymbol{a}_r(\theta_{k^*}^r)^H \boldsymbol{H} \boldsymbol{a}_t(\theta_{k^*}^t)\sqrt{E}s^*|^2 > \\ &\quad |\boldsymbol{y}_c(\hat{k}) - \boldsymbol{a}_r(\theta_{\hat{k}}^r)^H \boldsymbol{H} \boldsymbol{a}_t(\theta_{\hat{k}}^t)\sqrt{E}\hat{s}|^2\big). \end{aligned} \tag{7}$$

For $k = k^*$ or $\hat{k}$ and $s = s^*$ or $\hat{s}$, we have $\boldsymbol{a}_r(\theta_k^r)^H \boldsymbol{H} \boldsymbol{a}_t(\theta_k^t)$ $\sqrt{E}s = \beta_k \sqrt{E}s$ according to the orthogonality assumptions provided in (2). Thus, we have

$$\boldsymbol{y}_c(k) = \boldsymbol{a}_r(\theta_k^r)^H \boldsymbol{y} = \begin{cases} \boldsymbol{a}_r(\theta_k^r)^H \boldsymbol{n}, & k \neq k^* \\ \beta_{k^*}\sqrt{E}s^* + \boldsymbol{a}_r(\theta_{k^*}^r)^H \boldsymbol{n}, & k = k^*. \end{cases}$$

Also, Eq. (7) is given by (8) at the top of the next page. We need to consider two different cases, i.e., $\hat{k} = k^*$ and $\hat{k} \neq k^*$.

A. CPEP with $\hat{k} = k^*$

When $\hat{k} = k^*$, detection of a transmission direction is correct, whereas the error comes from $\hat{s} \neq s^*$. Thus, combining Eqs. (7) and (8), we have

$$\begin{aligned} &\mathbb{P}\big(\{k^*, s^*\} \to \{k^*, \hat{s}\} \mid \beta_1, \ldots, \beta_{N_s}\big) = \\ &\mathbb{P}\big(|\boldsymbol{a}_r(\theta_{k^*}^r)^H \boldsymbol{n}|^2 \ > \ |\beta_{k^*}\sqrt{E}(s^* - \hat{s}) + \boldsymbol{a}_r(\theta_{k^*}^r)^H \boldsymbol{n}|^2\big) = \\ &\mathbb{P}\big(2\Re\big[\boldsymbol{n}^H \boldsymbol{a}_r(\theta_{k^*}^r)\beta_{k^*}\sqrt{E}(s^* - \hat{s})\big] + |\beta_{k^*}\sqrt{E}(s^* - \hat{s})|^2 < 0\big). \end{aligned}$$

Let $w = 2\Re\big[\boldsymbol{n}^H \boldsymbol{a}_r(\theta_{k^*}^r)\beta_{k^*}\sqrt{E}(s^* - \hat{s})\big] + |\beta_{k^*}\sqrt{E}(s^* - \hat{s})|^2$, then we have $w \sim \mathcal{N}(\mu_w, \sigma_w^2)$, where $\mu_w = |\beta_{k^*}|^2 E|s^* - \hat{s}|^2, \sigma_w^2 = 2\sigma^2|\beta_{k^*}|^2 E|s^* - \hat{s}|^2$. Thus,

$$\mathbb{P}\big(\{k^*, s^*\} \to \{k^*, \hat{s}\}|\beta_1, \ldots, \beta_{N_s}\big) = Q\left(\sqrt{\frac{|\beta_{k^*}|^2 E|s^* - \hat{s}|^2}{2\sigma^2}}\right) \tag{9}$$

where $Q(\cdot)$ denotes the Q-function.

B. CPEP with $\hat{k} \neq k^*$

When $\hat{k} \neq k^*$, detection of transmission direction is incorrect. In this case, we have either $\hat{s} \neq s^*$ or $\hat{s} = s^*$. Thus, again combining Eqs. (7) and (8), we have

$$\begin{aligned} &\mathbb{P}\big(\{k^*, s^*\} \to \{\hat{k}, \hat{s}\} \mid \beta_1, \ldots, \beta_{N_s}\big) = \\ &\mathbb{P}\big(|\boldsymbol{a}_r(\theta_{k^*}^r)^H \boldsymbol{n}|^2 \ > \ |\boldsymbol{a}_r(\theta_{\hat{k}}^r)^H \boldsymbol{n} - \beta_{\hat{k}}\sqrt{E}\hat{s}|^2\big). \end{aligned}$$

Let $w_1 \triangleq |\boldsymbol{a}_r(\theta_{k^*}^r)^H \boldsymbol{n}|^2$ and $w_2 \triangleq |\boldsymbol{a}_r(\theta_{\hat{k}}^r)^H \boldsymbol{n} - \beta_{\hat{k}}\sqrt{E}\hat{s}|^2$. Since $\boldsymbol{a}_r(\theta_{k^*}^r)^H \boldsymbol{n} \sim \mathcal{CN}(0, \sigma^2)$, $\frac{w_1}{\sigma^2/2}$ is a chi-squared random variable with two degrees of freedom, which has an exponential distribution with the rate $1/2$. For w_2, since $\boldsymbol{a}_r(\theta_{\hat{k}}^r)^H \boldsymbol{n} - \beta_{\hat{k}}\sqrt{E}\hat{s} \sim \mathcal{CN}(-\beta_{\hat{k}}\sqrt{E}\hat{s}, \sigma^2)$, $\frac{w_2}{\sigma^2/2}$ is distributed as a non-central chi-squared random variable with two degrees of freedom and the non-centrality parameter $\lambda = \frac{2|\beta_{\hat{k}}|^2 E|\hat{s}|^2}{\sigma^2}$. Also, with the assumption in (2), we have $\boldsymbol{a}_r(\theta_{k^*}^r)^H \boldsymbol{a}_r(\theta_{\hat{k}}^r) = 0$, so that $\boldsymbol{a}_r(\theta_{k^*}^r)^H \boldsymbol{n}$ are independent of $\boldsymbol{a}_r(\theta_{\hat{k}}^r)^H \boldsymbol{n}$ [10], which implies that w_1 is independent of w_2. With all these properties, we have the following probability after some manipulations:

$$\mathbb{P}\big(\{k^*, s^*\} \to \{\hat{k}, \hat{s}\} \mid \beta_1, \ldots, \beta_{N_s}\big) = \frac{1}{2} e^{\left(-\frac{|\beta_{\hat{k}}|^2 E|\hat{s}|^2}{2\sigma^2}\right)}. \tag{10}$$

C. Bit Error Rate

With the CPEPs in Eqs. (9) and (10), we derive the BER using the union bound as follows:

$$\begin{aligned} &p_b(\beta_1, \ldots, \beta_{N_s}) \leq \frac{1}{N_b N(k^*, s^*)} \sum_{k^*, s^*} \sum_{\hat{k}, \hat{s}} \\ &\mathbb{P}\big(\{k^*, s^*\} \to \{\hat{k}, \hat{s}\} \mid \beta_1, \ldots, \beta_{N_s}\big) E_b\big(\{k^*, s^*\} \to \{\hat{k}, \hat{s}\}\big) \end{aligned} \tag{11}$$

where N_b is the total number of bits (included in both the direction and the symbol) transmitted every time, $N(k^*, s^*)$ is the total number of possible realizations of k^* and s^*, and $E_b\Big(\{k^*, s^*\} \to \{\hat{k}, \hat{s}\}\Big)$ is the number of erroneous bits when k^*, s^* are transmitted but $\hat{k}, \hat{s}$ are received.

Using the same example as in Section II-C, we have $N_b = 4$. For four possible transmission directions (k^*) and four possible transmitted symbols (s^*), there are total $4 \times 4 = 16$ possible realizations of k^* and s^*, thus $N(k^*, s^*) = 16$. If $k^* = 1, s^* = \frac{1+1j}{\sqrt{2}}\big([b_1, b_2, b_3, b_4] = [0000]\big)$, and detected $\hat{k} = 2, \hat{s} = \frac{1-1j}{\sqrt{2}}\big([\hat{b}_1, \hat{b}_2, \hat{b}_3, \hat{b}_4] = [0101]\big)$, then two bits are incorrect so that $E_b\Big(\{k^*, s^*\} \to \{\hat{k}, \hat{s}\}\Big) = 2$ in this case. From the example, we see that the BER performance (11) is related to not only the CPEP of error events, but also the number of scattering clusters chosen as candidate transmission directions and the size of symbol modulation.

IV. Simulation Results

We compare our transmission scheme with other two schemes: maximum beamforming (MBF), where the UT steers to the scattering cluster with the largest gain β_1, and the random beamforming (RBF), where the UT steers to one of N_s clusters randomly. We assume both the UT and BS have 32 antennas $N_t = N_r = 32$, and four RF chains at the BS, that is, $R = 4$. The spacing between antennas is set to be $d_t = d_r = \frac{\lambda}{2}$. Each of N_{ts} scattering clusters has gain $\beta_l, l = 1, \ldots, N_{ts}$, distributed by $\beta_l \sim \mathcal{CN}(0, 1)$, and we choose $N_s = 4$ largest $|\beta_l|$ and use corresponding scattering clusters to implement the SSM scheme. For simplicity, the AoA and AoD corresponding to each cluster are uniformly chosen from DFT bins, so that the orthogonality among array vectors is guaranteed. For fair comparisons, we fix the spectral efficiency for different schemes to four bits per transmission. Since the SSM utilizes $N_s = 4$ scattering clusters, the symbol s is modulated using quadrature phase shift keying (QPSK),

$$
\begin{aligned}
|\boldsymbol{y}_c(k^*) - \boldsymbol{a}_r(\theta^r_{k^*})^H \boldsymbol{H} \boldsymbol{a}_t(\theta^t_{k^*}) \sqrt{E} s^*|^2 &= |\boldsymbol{a}_r(\theta^r_{k^*})^H \boldsymbol{n}|^2 \text{ and} \\
|\boldsymbol{y}_c(\hat{k}) - \boldsymbol{a}_r(\theta^r_{\hat{k}})^H \boldsymbol{H} \boldsymbol{a}_t(\theta^t_{\hat{k}}) \sqrt{E} \hat{s}|^2 &= \begin{cases} |\boldsymbol{a}_r(\theta^r_{\hat{k}})^H \boldsymbol{n} - \beta_{\hat{k}} \sqrt{E} \hat{s}|^2, & \hat{k} \neq k^* \\ |\beta_{k^*} \sqrt{E}(s^* - \hat{s}) + \boldsymbol{a}_r(\theta^r_{k^*})^H \boldsymbol{n}|^2, & \hat{k} = k^*. \end{cases}
\end{aligned} \tag{8}
$$

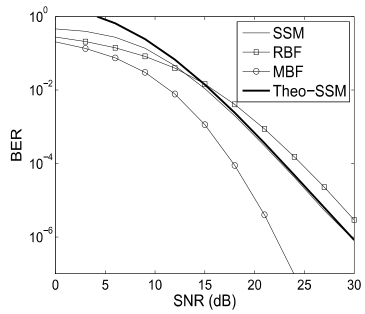

Fig. 2. BER performance with $N_{ts} = 6$.

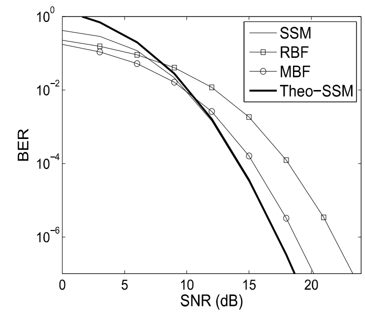

Fig. 3. BER performance with $N_{ts} = 12$.

which overall gives four bits per transmission. In contrast, the MBF and RBF use 16 quadrature amplitude modulation (16-QAM).

Figs. 2 and 3 show the BER performance of three schemes with $N_{ts} = 6$ and $N_{ts} = 12$, as well as the derived theoretical bounds on the BER for the SSM, denoted by Theo-SSM. We can observe the following facts:

- The derived bound is tight in the high SNR range.
- When the total number of scattering clusters is large, e.g., $N_{ts} = 12$, the proposed SSM scheme can achieve better BER performance over the MBF and RBF. MBF can achieve the largest instantaneous SNR due to steering to the cluster which has the largest gain. There are no errors in detecting the transmission directions since the receiver knows the transmission direction and forms beam towards the scattering cluster corresponding to the transmission scattering cluster. However, since the SSM explores the additional spatial dimension to modulate information bits, it can achieve the same spectral efficiency as the MBF and RBF using smaller modulation constellations, for example, QPSK vs. 16QAM in the simulation.
- When gains of different scattering clusters are similar to each other, the benefit from using smaller constellations will exceed the loss of not steering to the cluster which has the largest gain. When N_{ts} is large, it is more likely to get N_s samples relatively large in magnitude, and thus SSM shows the advantage over other two schemes.

Notice that as the number of antennas increases, we have a finer spatial resolution and will be able to distinguish more scattering clusters. Also it has been reported that for some indoor transmission environments, a large number of observed scattering clusters (including multiple reflections) exists in the 60 GHz mmWave frequency [11], [12].

V. Conclusions

In this paper, we have proposed a new spatial scattering modulation for uplink mmWave communication systems. An analog beamforming and hybrid beamforming have been employed at the UT and BS to reduce the number of RF chains. The proposed SSM has leveraged this architecture to utilize the spatial dimension, inherent to the mmWave channel, to modulate additional information bits. Comparing to other transmission schemes such as MBF and RBF that also use this architecture, the simulation results have shown that since smaller modulation constellations can be used the proposed SSM results in better BER performance when the number of scattering clusters is large.

References

[1] R. W. Heath, *et al.*, "An overview of signal processing techniques for millimeter wave MIMO systems," *IEEE J. Sel. Topics Signal Process.*, vol. 10, no. 3, pp. 436–453, 2016.

[2] H. L. Van Trees, *Detection, estimation, and modulation theory, optimum array processing*. John Wiley & Sons, 2004.

[3] R. Y. Mesleh, *et al.*, "Spatial modulation," *IEEE Trans. Veh. Technol.*, vol. 57, no. 4, pp. 2228–2241, 2008.

[4] P. Liu and A. Springer, "Space shift keying for los communication at mmwave frequencies," vol. 4, no. 2, pp. 121–124, 2015.

[5] N. Ishikawa, R. Rajashekar, S. Sugiura, and L. Hanzo, "Generalized spatial modulation based reduced-RF-chain millimeter-wave communications," *IEEE Trans. Veh. Technol.*, vol. 66, no. 1, pp. 879–883, 2017.

[6] A. M. Sayeed, "Deconstructing multiantenna fading channels," *IEEE Trans. Signal Process.*, vol. 50, no. 10, pp. 2563–2579, 2002.

[7] O. El Ayach, *et al.*, "Spatially sparse precoding in millimeter wave MIMO systems," *IEEE Trans. Wireless Commun.*, vol. 13, no. 3, pp. 1499–1513, 2014.

[8] S. Sun, *et al.*, "MIMO for millimeter-wave wireless communications: beamforming, spatial multiplexing, or both?" *IEEE Commun. Mag.*, vol. 52, no. 12, pp. 110–121, 2014.

[9] X. Zhang, A. F. Molisch, and S.-Y. Kung, "Variable-phase-shift-based RF-baseband codesign for MIMO antenna selection," *IEEE Trans. Signal Process.*, vol. 53, no. 11, pp. 4091–4103, 2005.

[10] D. Tse and P. Viswanath, *Fundamentals of wireless communication*. Cambridge university press, 2005.

[11] A. Maltsev, *et al.*, "Experimental investigations of 60 GHz WLAN systems in office environment," *IEEE J. Sel. Areas Commun.*, vol. 27, no. 8, pp. 1488–1499, 2009.

[12] A. Maltsev *et al.*, "Channel models for 60 GHz WLAN systems," [Online]. Available: https://mentor.ieee.org/802.11/dcn/09/11-09-0334-08-00ad-channel-models-for-60-ghz-wlan-systems.doc, May 2010.